



Cite this: *RSC Appl. Polym.*, 2024, **2**, 880

## Improving the *in vivo* stability and sensor lifetime with new blend membranes on CGM sensors†

Yinxu Zuo, Lanjie Lei, Ke Huang, Qing Hao, Chao Zhao  and Hong Liu  \*

Continuous glucose monitoring (CGM) is essential for managing diabetes, including closed-loop (artificial pancreas) technology. However, the current lifetime of commercial glucose sensors used in CGM based on the electrochemical method is limited to 3–15 days. The instability or failure of implanted electrochemical glucose sensors caused by tissue reactions, outer membrane degradation, calcification, and delamination can decrease *in vivo* sensor accuracy and lifetime. Durable outer membrane materials with good biocompatibility are crucial to improve the accuracy and durability of long-term implantable electrochemical glucose sensors *in vivo* and overcome these obstacles. This study used PDMS/HydroThane as the outer membrane of the glucose sensors to demonstrate long-term *in vivo* stability in non-diabetic dogs for 28 days. The good biocompatibility and stability of the outer membrane contributed to the extended sensor lifetime. Additionally, the study evaluated the effect of oxygen on the performance of glucose sensors coated with PDMS/HydroThane blending membranes containing different PDMS contents. The results showed that glucose sensors coated with blending membranes of PDMS/HydroThane with a weight ratio of 10 : 50 were essentially independent of environmental PO<sub>2</sub> while blending membranes of PDMS/HydroThane with a weight ratio of 5 : 50 coated glucose sensors were affected by oxygen fluctuation. This new membrane was developed to increase the *in vivo* lifetime of CGM sensors with quick response time and good *in vivo* stability and provide valuable insights into the design and development of new glucose sensors for long-term CGM applications.

Received 3rd April 2024,  
Accepted 28th June 2024  
DOI: 10.1039/d4lp00123k

rsc.li/rscapppolym

## Introduction

Diabetes mellitus, a metabolic disease affecting millions worldwide, can lead to impaired blood glucose control.<sup>1–4</sup> It is characterized by persistent hyperglycemia caused by imbalances in insulin secretion. The management of diabetes primarily relies on monitoring blood glucose levels to prevent complications such as cardiovascular diseases, neuropathy, and retinopathy. Continuous glucose monitoring (CGM) systems have emerged as a transformative technology in diabetes management, offering real-time observation of blood glucose fluctuations and enabling timely interventions. Unlike traditional finger-prick methods, CGM sensors provide continuous blood glucose monitoring data, which is crucial for optimizing therapy and improving glycemic control.<sup>5–7</sup> The application of CGM sensors has been shown to reduce glycated hemoglobin (HbA1c) levels, lower the risk of hypoglycemia, and enhance the overall quality of life for diabetic patients.<sup>8–10</sup>

The outer membranes of CGM sensors play a critical role in determining their functionality, affecting glucose permeability, oxygen permeability, biocompatibility, and stability.<sup>11</sup> The primary function of these membranes is to regulate the transport rate and proportion of glucose and oxygen to the sensor's active site while protecting the sensor from biofouling and enzymatic degradation.<sup>12,13</sup> Commercially available CGM sensors use various membrane formulations and strategies to enhance their performance and longevity. For example, polyurethane is one of the most commonly used materials in CGM sensor membranes due to its good biocompatibility, adjustable ratios of soft and hard segments, hydrophilic and hydrophobic properties, and mechanical properties.<sup>14</sup> The structure of polyurethane consists of soft and hard segments, and by adjusting their ratios, the flexibility and mechanical strength of polyurethane can be regulated. Polyurethane can also be modified by adjusting the ratios of hydrophilic and hydrophobic segments and incorporating PDMS for oxygen permeability, thereby controlling the sensor's biocompatibility, glucose and oxygen permeability, ultimately altering the sensor's stability and accuracy.<sup>15–17</sup>

Our research focuses on developing and applying a new blend membrane composed of polydimethylsiloxane (PDMS) and Hydrothane (HT) for CGM sensors. Hydrothane is a com-

State Key Laboratory of Bioelectronics, School of Biological Science and Medical Engineering, Southeast University, Nanjing 210096, China. E-mail: liuh@seu.edu.cn  
† Electronic supplementary information (ESI) available. See DOI: <https://doi.org/10.1039/d4lp00123k>



mercial thermoplastic polyurethane with good biocompatibility and tunable hydrophilic properties. Sensors modified with this blend membrane have been successfully applied in continuous glucose monitoring in beagles, demonstrating stable and continuous glucose measurements for over 28 days without significant sensitivity degradation. The excellent biocompatibility of the PDMS/HT blend membrane is likely the main reason for this outstanding performance. Additionally, we investigated the impact of varying PDMS content on sensor accuracy. Insufficient PDMS content can lead to reduced sensor sensitivity due to inadequate oxygen permeability, known as the “oxygen effect.” Conversely, the optimal PDMS content ensures sufficient oxygen permeability, maintaining sensor accuracy and preventing the sensitivity decline associated with the oxygen effect. These findings demonstrate the potential of PDMS/HT blend membranes to enhance the *in vivo* stability and longevity of CGM sensors, offering promising implications for improving the lifespan and performance of CGM sensors in diabetes management.

## Experiments

### Chemicals and materials

The HydroThane 80A (HT, water adsorption rate 25%) was provided by AdvanSource Biomaterials (Wilmington, USA). PDMS (viscosity: 12 500 cSt, medical grade) was obtained from Dow Corning (Michigan, USA). Bovine serum albumin (BSA) and GOx (from *Aspergillus niger*, 200 units per mg) were purchased from Sigma-Aldrich. Phosphate-buffered saline (PBS) was prepared in the lab. The glucose solution with different concentrations was prepared in the lab and calibrated with YSI 2500. D-(+)-Glucose, ascorbic acid (AA, 98%), uric acid (UA, 99%), and Acetaminophen (AP, 99%) were provided by Sigma-Aldrich (Shanghai, China). Tetrahydrofuran (THF) was obtained from Sinopharm Chemical Reagent Co., Ltd (Beijing, China). Saline solution (sterile, 0.9%) was purchased from Beyotime Biotechnology (Shanghai, China). Xylene, hematoxylin, and eosin were bought from Macklin (Shanghai, China). TNF- $\alpha$ , IL-1 $\beta$ , and IL-6 antibodies were provided by Thermo Fisher (Shanghai, China). Insulin aspart was purchased from Novo Nordisk (Denmark). Tissue glue was obtained from the 3M Cooperation Company (USA). A dextrose injection (50% concentration) was purchased from Nanyang Nude Trading Co., Ltd (Nanyang, China). PBS containing 1.9 mmol L<sup>-1</sup> NaH<sub>2</sub>PO<sub>4</sub>·H<sub>2</sub>O, 8.1 mmol L<sup>-1</sup> Na<sub>2</sub>HPO<sub>4</sub>·12H<sub>2</sub>O, 138.0 mmol L<sup>-1</sup> NaCl, 2.7 mmol L<sup>-1</sup> KCl, and 1.0 mmol L<sup>-1</sup> EDTA was prepared in the lab. The pH of PBS was adjusted to 7.4 using HCl or NaOH. A Millipore Milli-Q Plus water purification system generated deionized water (18.2 M $\Omega$  cm<sup>-1</sup>). Unless otherwise specified, all reagents were used as received without further purification.

### Material characterization

A metallographic microscope was used to measure the thickness of the blended polymer membrane (Huiguang

Technology Co. Ltd). The surface morphology of the membrane was observed using a FEI Inspect F scanning electron micrographs (SEM) device operating at a 2 kV acceleration voltage, and the membrane was sputtered with gold before observation. To perform the strain–stress experiments, polymer samples with a thickness of 2 mm were made from a polymer solution in THF. They cut into the dimensions of a dumbbell (115 mm in length and 25 mm in breadth, with a narrow segment measuring 33 mm in length and 6 mm in width). These samples were tested utilizing a Single Column Motor Table (Shenzhen Suns Technology Stock Co. Ltd) with an upper force limit of 50 N and a force ramp rate of 5 N min<sup>-1</sup>. In the water sorption test, the membrane was submerged in PBS (0.1 M) for 72 hours, surplus water was blotted using filter paper, and the amount absorbed was calculated by weighing the films. Using the following formula, the water sorption rate was calculated as a percentage of membrane weight gain or  $D_w$ :

$$D_w = \left( \frac{W_s - W_d}{W_d} \right) \times 100\%$$

the weight of membranes before and after immersion was denoted as  $W_d$  and  $W_s$ , respectively.

Using a metallographic microscope to compare the membrane thickness before and after water adsorption allowed researchers to calculate the membrane expansion rate. The following formula was used to calculate the membrane expansion rate as a percentage of membrane thickness gain, or  $D_e$ :

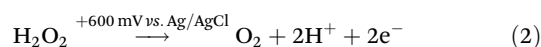
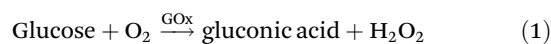
$$D_e = \left( \frac{E_s - E_d}{E_d} \right) \times 100\%$$

$E_d$  and  $E_s$  stand for the membrane's thickness before and after immersion.

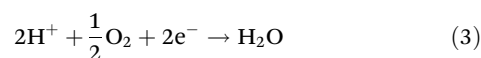
The response time was defined as the time needed to increase the glucose concentration from 5.0 to 10.0 mM and achieve 90% of the maximum response.

### Working mechanism

The amperometric sensor converts glucose molecules into hydrogen peroxide (H<sub>2</sub>O<sub>2</sub>), using glucose oxidase (GOx). Through a series of reactions, the concentration of H<sub>2</sub>O<sub>2</sub> is detected on the surface of the working electrode (WE) when a bias of +0.6 V is applied anodically.<sup>18,19</sup>



The reduction reaction balances the current flow at the counter electrode (CE).



To prevent undesired saturation effects in glucose measurement, it is crucial to maintain excess oxygen compared to glucose at the WE surface. Oxygen plays an essential role in



the reaction (1). Electroactive materials, such as uric acid and ascorbic acid, are commonly found in the interstitial fluid (IF) and contribute to the total current at +0.6 V, which interferes with the detection of hydrogen peroxide and results in an inaccurate glucose reading. To ensure the sensor's proper functioning and selectivity, inner membranes are placed at the WE. Additionally, a reference electrode is required to maintain the WE potential fixed, which is essential for the sensor to remain stable and produce consistent results over time.<sup>20</sup>

The hydrophilicity of the PDMS/HT blending membrane is provided by HT. The hydrophilic part of HT allows glucose to diffuse through it, while the high permeability of PDMS to oxygen<sup>21</sup> gives the blending membrane good oxygen permeability. By adjusting the content of PDMS and HT in the outer membrane, the diffusion of glucose and oxygen can be regulated, reducing the sensor's dependence on oxygen and increasing the response linearity. This membrane offers several advantages, including improved performance and longevity of subcutaneously implanted sensors. It also protects glucose oxidase at the electrode, preventing proteins and other substances from moving toward the electrode. Furthermore, since this membrane is in direct contact with subcutaneous tissue, it plays a critical role in determining the biocompatibility of the sensor.<sup>22,23</sup>

The PDMS/HydroThane blending polymer can form a stable blending membrane that may be attributed to the following reasons. First, the van der Waals forces contribute to the overall interaction between PDMS and HydroThane. Although these forces are not very strong individually, collectively, they can help maintain the stability of the blending polymer. Second, the surface energy and wetting between PDMS and HydroThane. Hydrophilic HydroThane has higher surface energy than hydrophobic PDMS. Ensuring good wetting of PDMS by HydroThane is crucial for intimate contact and strong interfacial adhesion. Third, forming interpenetrating polymer networks (IPNs) involves the interdiffusion and entanglement of polymer chains from both PDMS and HydroThane at the molecular level. This can be facilitated by controlling the curing and processing conditions, ensuring that the polymers interpenetrate and form a stable, cohesive network.

### Sensor design

Zhejiang POCTech Co. Ltd/Jiangsu Yuekai Biotech provided the sensors without outer membrane coating. A polyimide (PI) substrate with a diameter of 250  $\mu\text{m}$  was used, with screen-printed platinum, Ag/AgCl, and gold as the working electrode, reference electrode, and counter electrode. The inner membrane and enzyme layer were formed according to previous reports.<sup>24,25</sup> Generally speaking, the enzyme layer was deposited on the electrode by spraying and crosslinked in glutaraldehyde vapor (produced from 25 wt% glutaraldehyde) for 15 min. The enzyme composition comprised 1.0 mL PBS (0.1 M), 50 mg GOx, and 36 mg BSA.<sup>26</sup>

The PDMS/HT outer membrane was added using a film coating apparatus (provided by Zhejiang POCTech Co. Ltd/Jiangsu Yuekai Biotech.). The procedures for the outer mem-

brane fabrication processes are as follows. First, tetrahydrofuran (THF) solution containing 5 wt% HydroThane (HT) and 5 wt% PDMS, respectively, were prepared, and they were mixed at different ratios to obtain the PDMS/HT blending polymer solution. Second, a film coating apparatus was used to fabricate the outer membrane for the CGM. The liquid film of the outer membrane polymer started from the distal end of the sensor, and by passing the sensor through a wire loop, the entire sensor was uniformly coated with the outer membrane. The sensor was then allowed to dry in the air for 5 minutes. The outer membrane fabrication process was halted until the sensor sensitivity reached 2.0–4.0 nA mM<sup>-1</sup>.

### Biocompatibility test

Rat skin tissue samples were taken after the sensor was implanted for 28 days to assess the tissue reactions to the implanted glucose sensor during continuous monitoring. The biocompatibility experiments used male Sprague-Dawley rats (SIVZ, Tierspital, Zurich, Switzerland) weighing 150–200 g. The glucose sensors were implanted under the rats' skin using a half-wall needle. The control and experimental groups were identified as the skin tissue surrounding the silicone and PDMS/HT blended membrane-coated glucose sensors, respectively. In contrast, the sham group was identified as the skin tissue surrounding the glucose sensors without an outer membrane.<sup>27,28</sup> The biocompatibility tests were performed using hematoxylin and eosin (HE) and immunohistochemistry (IHC) stains, as previously reported.<sup>29,30</sup>

### In vivo glucose sensing

All animal experiments were carried out according to the National Institutes of Health Guide for the Care and Use of Laboratory Animals and were approved by the Scientific Ethical Committee of Southeast University. For this experiment, three beagles weighing over 15 kg were utilized. Sensors were placed on each beagle's neck using the supplied applicator and following the manufacturer's recommended procedures (Yuwell CT2A CGM). It's important to note that, apart from modifying the outer membrane, all other steps were completed in the same manner as the commercially available Yuwell CT2A CGM sensors, including assembly, packaging, and sterilization. Therefore, these prepared glucose sensors were assembled and sealed in sterile packaging and sent to CGN Irradiation Technology Co. Ltd for sterilization using electron-beam radiation with a dosage of 25 kGy. Other necessary components for continuous glucose monitoring, such as transmitters, batteries, and tapes, are also available from Zhejiang POCTech Co. Ltd/Jiangsu Yuekai Biotech. Therefore, the sensor application process used in this experiment is identical to that of the commercial CT2A CGM sensors.

Before application, the hair around the beagle's neck was clipped, and the skin was cleaned with alcohol. A drop of tissue glue was placed on the skin-facing surface of the double-sided tape on glucose sensors. After the application, the transmitters with new batteries installed were used and connected to the app for continuous glucose monitoring. To



prevent the sensors' removal, the beagles' necks wore an elastic bandage during the test period. The CGM system's initial calibration was performed approximately 1 hour after sensor implantation.

CGMS data was collected during the glycemic clamp state in this experiment. The glycemic clamp technique is a method used to quantify beta-cell sensitivity to glucose and tissue sensitivity to insulin.<sup>31</sup> It was used to create hyperglycemic and hypoglycemic conditions to calculate the *in vivo* sensitivity of implanted glucose sensors. The overall *in vivo* test lasted for 31 days, and the glycemic clamp state was generated on days 3, 15, 28, and 31. The beagles were fed once daily with food and water. Interstitial glucose concentration was determined using our glucose sensor and a veterinary glucometer (Tara, Abbott) for comparison.

The CGM sensors were calibrated using a one-point calibration procedure based on the results using blood glucose test strips. This process involved converting the time-dependent current signal ( $i(t)$ ) to blood glucose concentration at a given time ( $C_G(t)$ ). Sensor sensitivity ( $S$ ) could also be determined using the calibration procedure, which was the slope of the calibration curve, representing the ratio between the current signal and the blood glucose concentration. To this end, discrete blood glucose measurements were taken in parallel from the cephalic vein pricks using veterinary glucometer strips (Tara, Abbott) every 6 minutes. Glucose concentrations from the cephalic vein blood were compared with sensor output during clamping. Approximately 30 groups of data related to blood glucose concentration and sensor output current were obtained, and the sensitivities were calculated based on linear regression fitting of data and obtained using the following equation:

$$S = \frac{I}{C}$$

$I$  and  $C$  represent the sensor response current and the blood glucose concentration.

### Data collection

Three beagles were implanted with sensors, and approximately 3 days after implantation, the glycemic clamp technique was applied in multiple phases. The clamp technique involved baseline glucose infusions during euglycemia, followed by the initiation of hyperglycemia (approximately 300 mg dL<sup>-1</sup>) for approximately 1 hour, then the initiation of hypoglycemia (approximately 50 mg dL<sup>-1</sup>) for approximately 1 hour, followed by the return to midrange glucose concentration (approximately 150 mg dL<sup>-1</sup>) and maintained for approximately 1 hour. The glucose infusions were then discontinued. An 18-gauge, 3.8 cm catheter was inserted into a cephalic vein to infuse dextrose and insulin.

The experiments started by administering 20% dextrose, prepared by diluting 50% dextrose in a saline solution. The infusion was given at different rates to achieve specific glycemic targets within 60 minutes. The insulin was mixed with a

20% dextrose solution to make a concentration of 100 mU mL<sup>-1</sup>, and it was infused at a rate of 0.15 mU kg<sup>-1</sup> min<sup>-1</sup>.

The hyperglycemic phase began with an infusion of insulin (1.1 mU kg<sup>-1</sup> min<sup>-1</sup>) and 20% dextrose (2.5 mL kg<sup>-1</sup> h<sup>-1</sup>); infusion rates during the hyperglycemic phase ranged from 0 to 1.1 mU kg<sup>-1</sup> min<sup>-1</sup> for insulin and 0.2 to 16 mL kg<sup>-1</sup> h<sup>-1</sup> for 20% dextrose. The hypoglycemic phase began with an infusion of insulin (1.1 mU kg<sup>-1</sup> min<sup>-1</sup>), and an injection of 20% dextrose (0.5 mL kg<sup>-1</sup> h<sup>-1</sup>) was initiated once the blood glucose concentration reached 60 mg dL<sup>-1</sup>. Infusion rates during the hypoglycemic phase ranged from 0 to 1.1 mU kg<sup>-1</sup> min<sup>-1</sup> for insulin and 0 to 2 mL kg<sup>-1</sup> h<sup>-1</sup> for 20% dextrose. The mid-range phase began with an infusion of insulin (1.1 mU kg<sup>-1</sup> min<sup>-1</sup>) and 20% dextrose (1.5 mL kg<sup>-1</sup> h<sup>-1</sup>); infusion rates during the midrange phase ranged from 0.06 to 6 mU kg<sup>-1</sup> min<sup>-1</sup> for insulin and 0.2 to 4.4 mL kg<sup>-1</sup> h<sup>-1</sup> for 20% dextrose. Blood glucose concentrations were measured every 6 minutes during the baseline and periods of rapid changes in glucose concentrations. Blood samples were collected at each time point and measured using a glucometer. At the end of the experimental period, infusions were discontinued, and the beagles were fed, provided water, and returned to their runs. Approximately 3 hours after completion of the clamp technique, data from the CGMS were downloaded to a computer database.

Consensus error grid analyses were conducted to evaluate the clamp data collected.<sup>32</sup> The error grid comprises 5 zones (A through E), each with a different clinical implication. Zone A indicates no effect on clinical action, while zone B suggests altered clinical action that is unlikely to affect the outcome. In contrast, zone C indicates altered clinical action likely to affect the clinical outcome, while zone D implies an altered clinical action that could pose a serious medical risk. Finally, zone E suggests an altered clinical action that could have dangerous consequences.

## Results and discussion

### Characterization of PDMS/HT with different weight ratios

SEM was employed to analyze the surface morphology of PDMS/HT composites with varying weight ratios. The HT's smooth and flat surface shape is shown in Fig. 1a. Adding additional PDMS increases roughness in the PDMS/HT blending membrane. The blending membrane exhibited a porous morphology when the weight ratio of PDMS to HT was 20 : 50, as depicted in Fig. 1d. With the increase of PDMS content, the surface morphology of the blending membrane becomes more and more rough, which is mainly caused by the phase separation of PDMS and HT.<sup>33</sup>

The mechanical strength of the outer membrane plays a crucial role in the performance of implanted glucose sensors during extended periods of wear, as it directly impacts signal accuracy and stability. Consequently, an investigation was conducted to analyze the mechanical properties of the PDMS/HT blending polymer, considering different weight ratios of





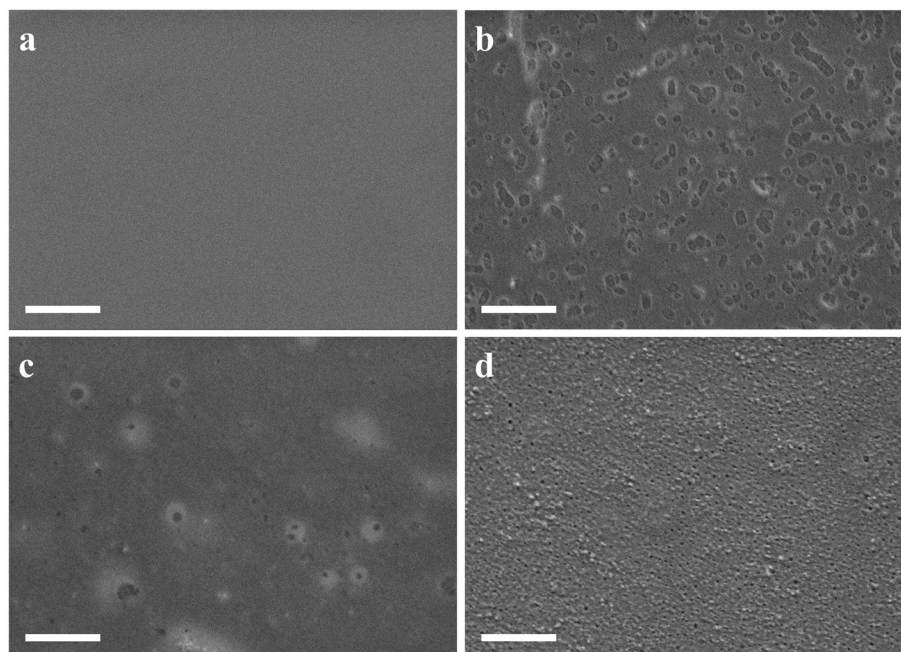


**Fig. 1** SEM images of the membrane: (a) HT; (b) PDMS/HT 5 : 50; (c) PDMS/HT 10 : 50; (d) PDMS/HT 20 : 50. Scale bar: 1  $\mu\text{m}$ , accelerating voltage: 2 keV.

PDMS. According to the data presented in Fig. S1,<sup>†</sup> it can be observed that the incorporation of PDMS resulted in a decrease in both the ultimate tensile strength and the elongation at break. This phenomenon can be attributed to the relatively low mechanical strength exhibited by PDMS compared with HT.<sup>33</sup>

#### ***In vitro* evaluation of oxygen effects on PDMS/HT outer membrane with different PDMS content coated glucose sensors**

The glucose concentration in interstitial fluid is higher than the oxygen concentration. To obtain accurate sensor output results, the outer membrane of CGM sensors should regulate the diffusion ratio of glucose/oxygen at a proper rate based on the electrooxidation of hydrogen peroxide.<sup>18</sup> PDMS is permeable to oxygen,<sup>21</sup> it was usually used in the outer membrane of TPU by blending or partially replacing the soft segment of TPU with PDMS.<sup>17</sup> However, the output signal of the CGM sensor depends on the concentration of oxygen instead of glucose if the content of PDMS is too low. The system was initially brought to air equilibrium to elucidate the relationship between PDMS content and the oxygen effect, and the glucose sensor baselines were stabilized. 10.0 mM of glucose was added to the system in two sequential injections, each providing a 5.0 mM concentration. This was 3.0–5.0 mM higher than the usual blood glucose level. A steady stream of  $\text{N}_2$  gas was added to the solution to lower the oxygen tension once the glucose sensors showed signs of stable current. This operation was done slowly while constantly stirring the solution to guarantee an oxygen balance throughout the cell. The oxygen

sensor was used to track the partial pressure of oxygen. The  $\text{N}_2$  flow was partially stopped to allow for a slow accumulation of oxygen in the system once the oxygen effect was noticed at a low  $\text{PO}_2$  level. This permitted the glucose sensors to start operating normally again. To achieve an accurate  $\text{PO}_2$  measurement at extremely low oxygen tension, the numerical values of the oxygen tension were also recorded simultaneously (as shown in Fig. 2a). One of the common data sets seen in the experiment mentioned above is Fig. 2. The oxygen partial pressure measured using a calibrated oxygen sensor is shown in Fig. 2a. Fig. 2b displays the current output of the CGM sensor (sensitivity: approximately  $3.8 \text{ nA mM}^{-1}$ ) coated with PDMS/HT blending outer membrane with a weight ratio of 5 : 50 in response to 10.0 mM glucose. Fig. 2c displays the output of the CGM sensor (sensitivity: approximately  $3.7 \text{ nA mM}^{-1}$ ) coated with PDMS/HT blending outer membrane with a weight ratio of 10 : 50. Interestingly, Fig. 2b shows that the sensor did not show any oxygen effect until the oxygen tension dropped to 8 mm Hg. At that point, the sensor began to function. It rapidly turned over due to the accumulated glucose trapped inside the enzyme layer's lack of  $\text{O}_2$  supply, producing a peak current before returning to the normal steady state current. Fig. 2c's CGM sensor demonstrates that it did not indicate any oxygen effect, even when the oxygen tension fell to 5 mm Hg.

Above all, when the weight ratio of PDMS/HT is 5 : 50, the oxygen effect may affect the accuracy of the output signal of the CGM sensor. When the weight ratio of PDMS/HT is 10 : 50, the oxygen effect does not exist. According to the SEM results, the porosity was observed in the blending membrane when the weight ratio of PDMS/HT is 20 : 50, which is detrimental to



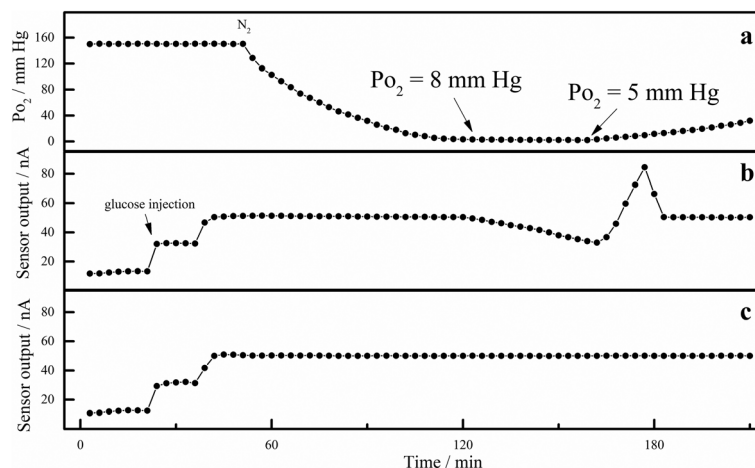


**Fig. 2** The oxygen effect of PDMS/HT blending membrane modified CGM sensor with different PDMS content, (a)  $PO_2$  in the system; (b) PDMS/HT with a weight ratio of 5 : 50 modified CGM sensors; (c) PDMS/HT with a weight ratio of 10 : 50 modified CGM sensors.

the long-term monitoring of CGM sensors, as the permeability of the sensor's outer membrane can lead to protein adsorption, thereby causing instability in the CGM sensors. In addition, the electrode and enzyme layer of the sensor are exposed to body fluids containing protein due to porosity, which rapidly degrades the sensor performance due to the contamination of the electrode and the deterioration of active enzymes. Therefore, PDMS/HT with a weight ratio of 10 : 50 was chosen in the following experiment.

#### Characterization of PDMS/HT with a weight ratio of 10 : 50

The water adsorption rate and membrane expansion rate of PDMS/HT (10 : 50) blending polymer were investigated, and results (Table S1†) show that the water adsorption rate was 27.4% and the membrane expansion rate was 32.5%.

The membrane thickness and the corresponding sensitivity were investigated. The results (Table S2†) show that the membrane thickness is  $44.7 \pm 1.5 \mu\text{m}$  when the sensitivity of the glucose sensor is  $3.88 \text{ nA mM}^{-1}$ . The metallographic figure of the membrane thickness is displayed in Fig. S2.† We can also see that the sensor's response time is 30 s, indicating that the sensor responds quickly to glucose.

For 28 days, the electrochemical stability of PDMS/HT outer membrane-coated glucose sensors was examined by comparing the sensitivity changes. At 1 h, 3 h, 6 h, 24 h, and daily intervals, the sensors' sensitivity was evaluated in glucose solutions with concentrations ranging from 0 to 30.0 mM (0, 5.0, 10.0, 15.0, 20.0, 25.0, and 30.0 mM) at  $32.0 \pm 0.5^\circ\text{C}$ . As shown in Fig. 3, the *in vitro* sensitivity rose from 1 h to 48 h and remained constant throughout the next testing days, which is explained by the electrode's surface stability.<sup>14</sup>

The chronoamperometric curve produced by testing PBS with different glucose concentrations ranging from 0 to 30.0 mM (0, 5.0, 10.0, 15.0, 20.0, 25.0, and 30.0 mM) at  $32.0 \pm 0.5^\circ\text{C}$  is shown in Fig. 4a and b. The current increased proportionately to the glucose concentration, showing a linear

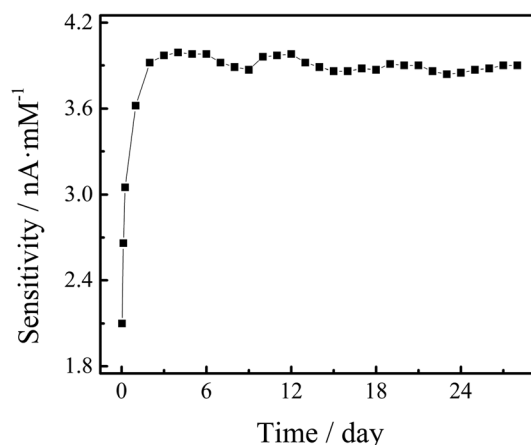


**Fig. 3** The stability test of PDMS/HT modified glucose sensors in PBS solution (pH 7.4, with different glucose concentrations from 0, 5.0, 10.0, 15.0, 20.0, 25.0, and 30.0 mM) at  $32.0 \pm 0.5^\circ\text{C}$  during 28 days. The stability was deemed as the sensitivity variations, and the sensitivity was calculated according to the slope of the current of the glucose sensors and glucose concentrations.

association with glucose concentration. A dose-response equation with a high correlation value of 0.9997 was obtained by linear regression analysis:  $i \text{ (nA)} = 9.0587 + 3.7120C \text{ (mmol L}^{-1}\text{)}$ . The glucose sensor's sensitivity was found to be  $3.7120 \text{ nA mM}^{-1}$ . Because of its adequate sensitivity and wide linear range, these results show that the developed glucose sensor satisfies the requirements for physiological glucose measurements.

Temperature changes profoundly affect both *in vitro* and *in vivo* sensor output current.<sup>34</sup> Therefore, the catalytic activity of glucose was assessed on PDMS/HT-coated sensors at different temperatures using amperometry. As seen in Fig. 4c, a steady-state current was obtained for a thermostatic 10.0 mM glucose solution at various temperatures ( $30.0 \pm 0.5$ ,  $33.0 \pm 0.5$ ,  $36.0 \pm 0.5$ ,  $39.0 \pm 0.5$ , and  $42.0 \pm 0.5^\circ\text{C}$ ). As seen in Fig. 4d, two



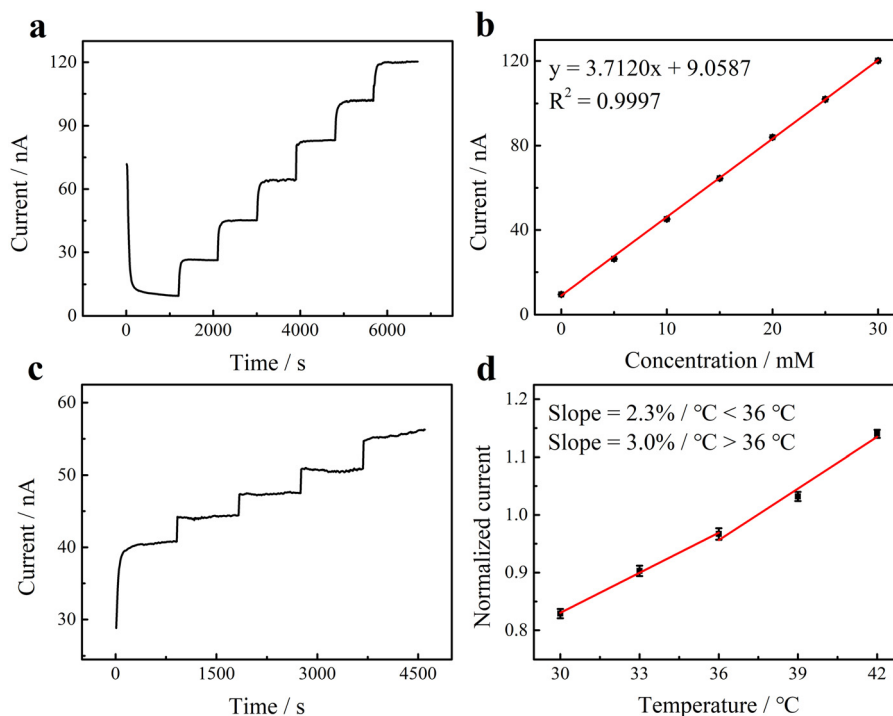


**Fig. 4** (a) Change in the sensor response with the sequential addition of glucose aliquots. Sensors were immersed in PBS (pH 7.4) at  $32.0 \pm 0.5$  °C while aliquots of glucose were added to produce step responses: 0, 5.0, 10.0, 15.0, 20.0, 25.0, and 30.0 mM. (b) Plot of calibrated sensor response as a function of glucose concentration. (c) Amperometric  $i-t$  curve of the sensor in 0.1 M PBS (pH 7.4) containing 10.0 mM glucose with different testing temperatures ( $30.0 \pm 0.5$ ,  $33.0 \pm 0.5$ ,  $36.0 \pm 0.5$ ,  $39.0 \pm 0.5$ , and  $42.0 \pm 0.5$  °C). (d) Temperature effect for glucose detection on PDMS/HT modified electrode.

temperature parameters of  $2.3\% \text{ } ^\circ\text{C}^{-1}$  ( $<36$  °C) and  $3.0\% \text{ } ^\circ\text{C}^{-1}$  ( $>36$  °C) were recorded. For the sake of comparison, the current was normalized to 37 °C.

In this work, acetaminophen (0.17 mM), bovine serum albumin ( $22 \text{ mg mL}^{-1}$ ),<sup>35</sup> physiological concentrations of L-ascorbic acid (0.11 mM)<sup>36</sup> and uric acid (0.48 mM)<sup>37</sup> are combined with 10.0 mM glucose in PDMS/HT-coated glucose sensors to examine the effects of recognized interferents. The PDMS/HT-modified glucose sensor demonstrates high selectivity for glucose detection, as shown in Fig. S3,† where the current change for glucose detection in the presence of possible interferents was less than 5%.

Electron beam radiation is a typical sterilizing procedure for implanted glucose sensors. The impact of electron beam radiation on sensor performance was thus investigated by contrasting the sensitivity variations before and after sterilization. The results are displayed in Table S3.† The results show that the sensitivity of the glucose sensors remained unchanged, indicating that the sterilizing procedure did not affect the polymer's permeability or the activity of the enzymes.

### Biocompatibility test

HE and IHC staining of rat tissues was used to assess the biocompatibility of the sensor. During prolonged use, the tissue reaction and sensor-associated fibrosis to electrodes are important variables influencing the sensor's accuracy and longevity.

Skin tissues surrounding the implanted sensor without an outer membrane were studied as part of a sham control group. In contrast, skin tissues surrounding the implanted sensor with PDMS/HT and silicone outer membrane were evaluated as experimental and control groups, respectively. Hematoxylin and eosin (H&E) staining results after 28 days of implantation showed that the tissues surrounding sensors with PDMS/HT (experimental group) outer membrane had thinner fibrous capsules (20  $\mu\text{m}$ ) and milder inflammatory cell infiltration than the tissues surrounding sensors without outer membrane (sham control group, 80  $\mu\text{m}$ ). Fig. 5 illustrates these findings. The silicone-coated sensors in the control group showed the least inflammatory cell infiltration and the thinnest fibrous capsules (12  $\mu\text{m}$ ). Additionally, IHC staining of IL-1 $\beta$ , IL-6, and TNF- $\alpha$  was performed to assess the inflammation in the skin tissue. The IHC staining revealed lower expression areas of IL-1 $\beta$ , IL-6, and TNF- $\alpha$  in the experimental group than in the sham groups and slightly higher than in the control group, as shown in Fig. 5b'-d'. These findings suggest that the outer membrane coating on glucose sensors has good biocompatibility.

### In vivo electrochemical glucose sensing

The *in vivo* stability and sensor lifetime of nine prepared CGM sensors coated with PDMS/HT outer membrane was evaluated in beagles over 31 days, and the detailed sensitivity variation





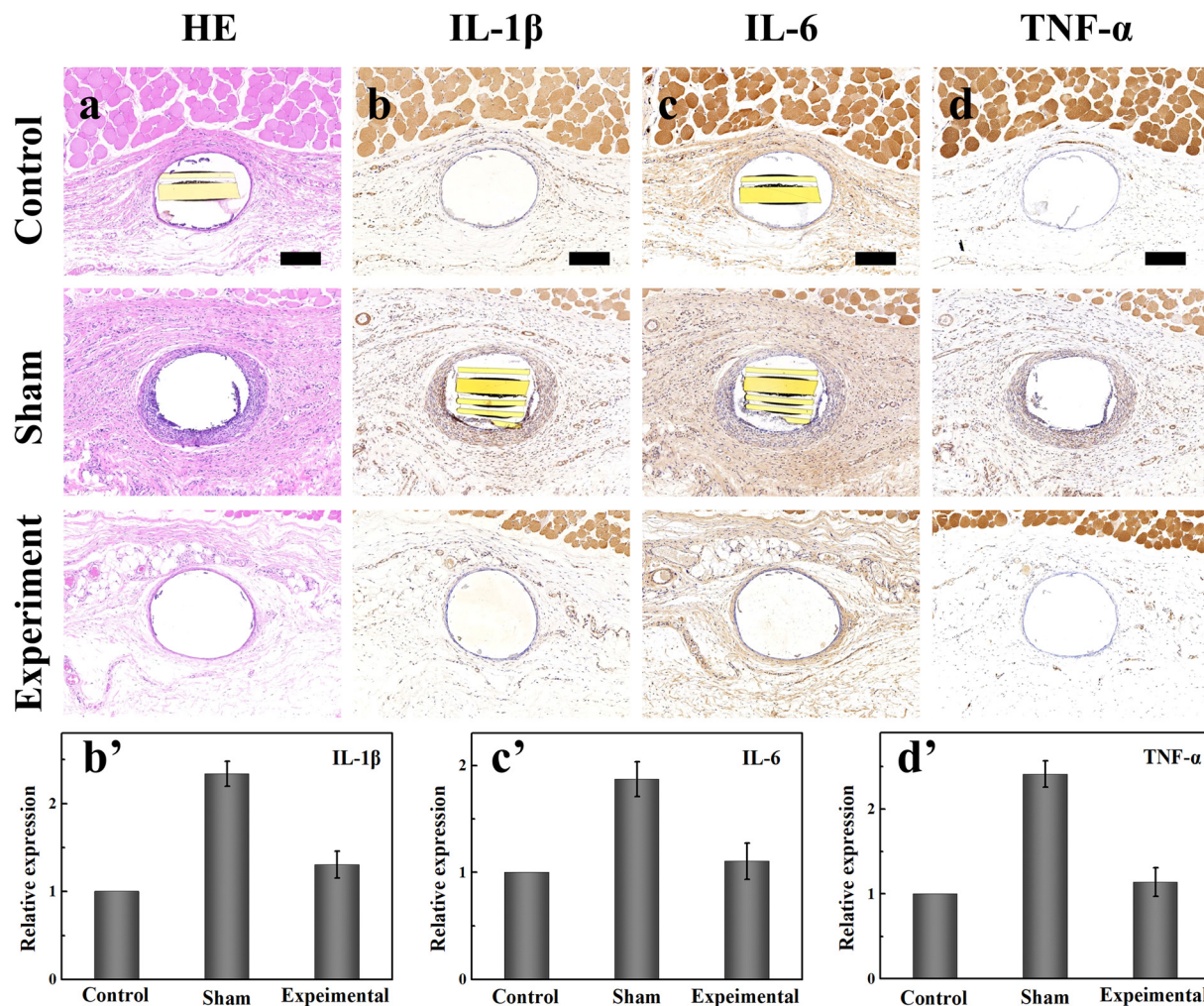


**Fig. 5** (a) HE staining micrographs of the skin tissues of the rats. (b–d) IHC of the IL-1β (b), IL-6 (c), and TNF-α (d) in the skin tissues. Grey-dyed cytokines could be observed in the tissues. (b'–d') Relative expression of the IL-1β (b'), IL-6 (c'), and TNF-α (d'). Scale bars: 200 μm. Control group: silicone-coated glucose sensors. Sham group: glucose sensors without outer membrane. Experiment group: PDMS/HT coated glucose sensors.

of the nine sensors on days 3, 15, and 28 was presented in Fig. S4† and Table 1. These results indicate that these sensors can work stably *in vivo* for more than 28 days. After 28 days, the implanted sensors commonly exhibited a progressive loss of sensor sensitivity until complete failure. The failure of sensors was likely due to tissue reactions of the sensor–tissue interface.<sup>38</sup> The mean *in vivo* sensitivity variation of the 9 sensors over time is shown in Fig. 6a, which remained rela-

tively stable during days 3 to 28. The stable *in vivo* performance of the implanted glucose sensors facilitates more concise output results, which is beneficial for advancing CGM management of diabetes. The sensor lifetime is extended for two weeks compared to some commercial CGM sensors, which can be attributed to the following reasons. First, the excellent biocompatibility of the outer membrane can reduce tissue reactions and prevent sensor-associated fibrosis. Second, the

**Table 1** *In vivo* sensitivity data obtained on different days

Sensor	Dog 1			Dog 2			Dog 3		
	1	2	3	4	5	6	7	8	9
Initial	3.89	3.87	3.85	3.82	3.80	3.88	3.85	3.82	3.89
Day 3	3.97	3.74	3.87	3.75	3.69	3.84	3.87	3.93	3.82
Day 15	3.65	3.63	3.88	3.68	3.67	3.84	3.80	3.90	3.88
Day 28	3.73	3.48	3.82	3.59	3.64	3.73	3.73	3.89	3.77
Day 31	1.79	2.24	2.53	2.36	1.98	2.32	2.45	2.38	2.26



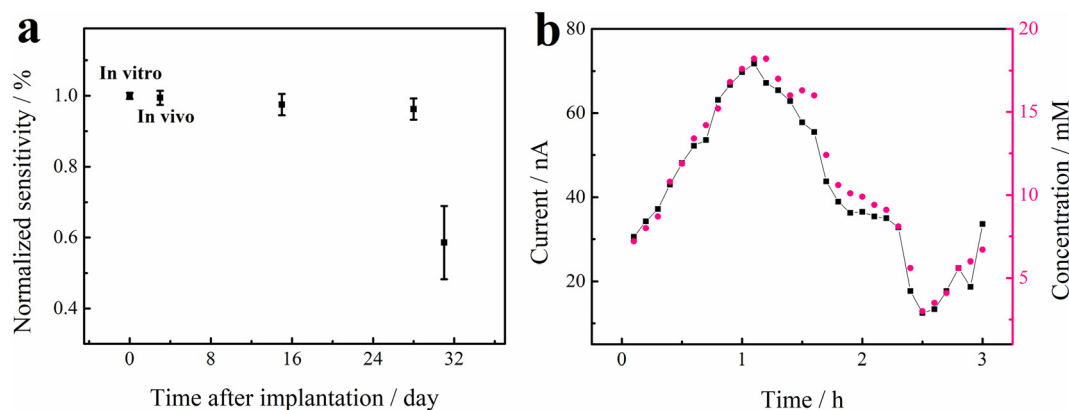


**Fig. 6** (a) Sensitivity *in vivo* of glucose sensors for 31 days. The data are the means of measurements from 9 sensors. Error bars are  $\pm$  SD. (b) Interstitial glucose concentrations (solid line) were obtained for one representative sensor during glycemic clamp procedures, and corresponding blood glucose concentrations (red circles) were concurrently measured using a veterinary glucometer method. Notice the lag between changes in blood glucose concentrations and CGMS values.

blending membrane has stable and reliable chemical/physical properties during long-term *in vivo* sensing without membrane degradation, leaching, segregation, or cracking.

The failure mechanism of CGM sensors after 31 days of implantation was investigated after the sensors were explanted from the beagles. The sensors were polarized in PBS after being explanted from beagles and tested in PBS with varying glucose concentrations. Results show that (Table S4†) the sensitivity of the explanted sensors was comparable to the initial *in vitro* sensitivity. These findings suggest that the progressive loss of sensor sensitivity and complete sensor failure were most likely due to the tissue reactions to the implanted sensor.<sup>28</sup>

During the glycemic clamp procedure, the lag time between CGMS values obtained from multiple concurrently implanted sensors and criterion-referenced values obtained from venous blood samples was found to be 9 minutes (Fig. 6b). The sensor itself accounted for 0.5 minutes of the signal delay, as determined from independent *in vitro* measurements, while an estimated 0.5 minutes was ascribed to circulatory transport from the central venous infusion site to the implant site.<sup>39</sup> The remaining delay of 7 minutes was attributed to mass transfer and physiological phenomena occurring within the local tissues. Notably, the lag time for blood and interstitial fluid glucose was included in the 7 minutes, and this delay value is consistent with findings from other studies.<sup>39,40</sup>

810 pairs of CGMS and criterion-referenced data were collected for analysis. Consensus grid analysis indicated that 88.0% of the measured values fell within zone A, while 12.0% were in zone B (Fig. S5 and Table S5†). No results were observed in zones C, D, or E. These findings suggest that the developed glucose sensor offers acceptable accuracy for ISF glucose measurements.

While previous reports have shown that the lifetime of glucose sensors has increased from 3 days to 15 days, there are few reports of sensors with reliable results beyond 15 days. In this work, the prepared CGM sensors can work *in vivo* for 28

days, extending the sensor lifetime by two weeks. These results suggest that the PDMS/HT blending membrane used in this work can potentially extend the lifetime of commercial CGM sensors by two weeks.

#### Long-term storage stability

In this study, the long-term storage stability of glucose sensors with an PDMS/HT outer membrane was thoroughly examined. The sensors typically exhibited a sensitivity range of 3.0–4.0 nA mM<sup>-1</sup> and maintained linearity between 5.0 and 30.0 mM, with a response time of 30 seconds following the injection of 5.0 mM glucose. The storage stability under ambient conditions (25.0  $\pm$  0.5 °C, RH 45%  $\pm$  5%) was evaluated after storage periods of 15, 30, 45, and 60 days. Before testing in glucose concentrations ranging from 5.0 mM to 30.0 mM, the sensors were polarized in PBS (pH 7.4) until the background current was reduced to below 10.0 nA. The background current was defined as the intercept of the linear regression analysis for the dose–response equation. Table 2 illustrates the change in sensitivity for these sensors before and after specific storage durations in ambient conditions. The results indicated only

**Table 2** Sensitivity changes before and after storage

	Before (nA mM <sup>-1</sup> )	After (nA mM <sup>-1</sup> )	Time of storage (day)	% change
1#	3.87	3.83	15	−1.0%
2#	3.85	3.81	15	−1.0%
3#	3.89	3.94	15	+1.3%
4#	3.76	3.82	30	+1.6%
5#	3.88	3.81	30	−1.8%
6#	3.82	3.73	30	−2.4%
7#	3.84	3.89	45	+1.3%
8#	3.79	3.68	45	−2.9%
9#	3.86	3.78	45	−2.1%
10#	3.85	3.93	60	+2.1%
11#	3.86	3.75	60	−2.8%
12#	3.88	3.79	60	+2.3%



minor signal changes ( $\leq 5\%$ ) within 60 days of storage in ambient conditions. These observations suggest that the bio-sensor possesses good storage stability, which can be attributed to the high chemical stability of the outer membrane and its protective effect on the electrode.

## Conclusion

This work demonstrated that PDMS/HT blending outer membrane can extend the sensor lifetime to at least 28 days with excellent *in vivo* stability when implanted subcutaneously in non-diabetic beagles, which extended the sensor life for 2 weeks compared with commercially used electrochemical implanted glucose sensors. It also evaluated the effect of oxygen on the blending membranes of PDMS/HT-coated glucose sensors with different PDMS content in the outer membrane. It demonstrated that glucose sensors coated with blending membranes of PDMS/HT with a weight ratio of 10:50 were essentially independent of environmental  $\text{PO}_2$  while blending membranes of PDMS/HT with a weight ratio of 5:50 coated glucose sensors were affected by oxygen fluctuation. This result is also important for developing a new outer membrane of implanted glucose sensors based on the electrochemical detection of hydrogen peroxide. This work provides a stable, protective membrane that can potentially be used for commercial long-term continuous glucose monitoring in diabetes management with an extended sensor lifetime.

## Author contributions

Yinxu Zuo: conceptualization, methodology, validation, investigation, data curation, writing – original draft, writing – review & editing. Lanjie Lei: methodology. Ke Huang: validation. Qing Hao: funding acquisition. Chao Zhao: funding acquisition. Hong Liu: conceptualization, data curation, supervision, funding acquisition.

## Data availability

The data supporting this study's findings are available from the corresponding author, upon reasonable request.

## Conflicts of interest

Authors have no conflict of interest to declare.

## Acknowledgements

We gratefully acknowledge financial support from the Key Research and Development Program of Jiangsu Province (BE2021700), National Natural Science Foundation of China (62001104, 62271136), National Key Research and

Development Plan (2022YFF1201803, 2021YFB2600800), Natural Science Foundation of Jiangsu Province (BK20200357), Science and Technology Development Program of Suzhou (SYG202117), Key Project and Open Research Fund of State Key Laboratory of Bioelectronics, the Fundamental Research Funds for the Central Universities (2242022R10052). We gratefully acknowledge the generous support and advice from Yanan Zhang and Zhejiang POCTech Co. Ltd/Jiangsu Yuekai Biotech for allowing us to use the CGM substrate platform, electrodes, data systems, and fabrication equipment for non-commercial purposes, which made this work possible. We gratefully acknowledge BioRender.com for allowing us to use the figures in the graphical abstract.

## References

- 1 A. S. Shah and K. J. Nadeau, *Diabetologia*, 2020, **63**, 683–691.
- 2 G. Xu, B. Liu, Y. Sun, Y. Du, L. G. Snetselaar, F. B. Hu and W. Bao, *BMJ [Br. Med. J.]*, 2018, **361**, 1497.
- 3 K. S. Kim, S. K. Kim, K. M. Sung, Y. W. Cho and S. W. Park, *Diabetes Metab. J.*, 2012, **36**(5), 336–344.
- 4 R. Ambady and S. Chamukuttan, *Rev. Endocr. Metab. Disord.*, 2008, **9**, 193–201.
- 5 C. M. Chen, L. C. Hung, Y. L. Chen and M. C. Yeh, *J. Clin. Nurs.*, 2018, **27**, 1673–1683.
- 6 S. R. Heller, *Diabetologia*, 2014, **57**, 847–849.
- 7 G. V. McGarraugh, W. L. Clarke and B. P. Kovatchev, *Diabetes Technol. Ther.*, 2010, **12**(5), 365–371.
- 8 G. Freckmann, J. H. Nichols, R. Hinzmann, D. C. Klonoff, Y. Ju, P. Diem, K. Makris and R. J. Slingerland, *Clin. Chim. Acta*, 2021, **515**, 5–12.
- 9 H. Gerstein, *Ann. Intern. Med.*, 2018, **168**(10), 53.
- 10 S. K. Garg, *Diabetes Technol. Ther.*, 2023, **25**, S1–S4.
- 11 S. P. Nichols, A. Koh, W. L. Storm, J. H. Shin and M. H. Schoenfish, *Chem. Rev.*, 2013, **113**, 2528–2549.
- 12 Y. Zou, Z. Chu, J. Guo, S. Liu, X. Ma and J. Guo, *Biosens. Bioelectron.*, 2023, **225**, 115103.
- 13 R. J. Soto, J. R. Hall, M. D. Brown, J. B. Taylor and M. H. Schoenfish, *Anal. Chem.*, 2017, **89**, 276–299.
- 14 B. Yu, N. Long, Y. Moussy and F. Moussy, *Biosens. Bioelectron.*, 2006, **21**(12), 2275–2282.
- 15 S. P. Nikam, P. Chen, K. Nettleton, Y. Hsu and M. L. Becker, *Biomacromolecules*, 2020, **21**(7), 2714–2725.
- 16 Y. Jung, S. Lee, J. Park and E. Shin, *Polymers*, 2022, **14**(20), 4269.
- 17 Q. Yan, T. C. Major, R. H. Bartlett and M. E. Meyerhoff, *Biosens. Bioelectron.*, 2011, **26**(11), 4276–4282.
- 18 A. Heller and B. Feldman, *Chem. Rev.*, 2008, **108**(7), 2482–2505.
- 19 C. Li, C. H. Ahn, L. A. Shutter and R. K. Narayan, *Biosens. Bioelectron.*, 2009, **25**(1), 173–178.
- 20 M. W. Shinwari, D. Zhitomirsky, I. A. Deen, P. R. Selvaganapathy, M. J. Deen and D. Landheer, *Sensors*, 2010, **10**(3), 1679–1715.



- 21 T. Goda, T. Konno, M. Takai, T. Moro and K. Ishihara, *Biomaterials*, 2006, **27**(30), 5151–5160.
- 22 G. S. Wilson and Y. Hu, *Chem. Rev.*, 2000, **100**(7), 2693–2704.
- 23 W. J. Sung, K. Na and Y. H. Bae, *Sens. Actuators, B*, 2004, **99**(2–3), 393–398.
- 24 Y. Zhang, Y. Hu, G. S. Wilson, D. Moatti-Sirat, V. Poitout and G. Reach, *Anal. Chem.*, 1994, **66**(7), 1183–1188.
- 25 Y. Zhang and G. S. Wilson, *Anal. Chim. Acta*, 1993, **281**(3), 513–520.
- 26 Y. Chen, B. Ma, Y. Zuo, G. Chen, Q. Hao, C. Zhao and H. Liu, *Biosens. Bioelectron.*, 2023, **235**, 115412.
- 27 H. Yoon, X. Xuan, S. Jeong and J. Y. Park, *Biosens. Bioelectron.*, 2018, **117**, 267–275.
- 28 J. I. Joseph, G. Eisler, D. Diaz, A. Khalf, C. Loeum and M. C. Torjman, *Diabetes Technol. Ther.*, 2018, **20**(5), 321–324.
- 29 L. Lei, C. Zhao, X. Zhu, S. Yuan, X. Dong, Y. Zuo and H. Liu, *Electroanalysis*, 2022, **34**, 415–422.
- 30 L. Yang, L. Lei, Q. Zhao, Y. Gong, G. Guan and S. Huang, *World J. Mens Health*, 2019, **37**, 186–198.
- 31 G. S. Meneilly and T. Elliott, *J. Am. Geriatr. Soc.*, 1998, **46**, 88–91.
- 32 J. L. Parkes, S. L. Slatin, S. Pardo and B. H. Ginsberg, *Diabetes Care*, 2000, **23**(8), 1143–1148.
- 33 Y. Du, J. Zhang and C. Zhou, *Polym. Bull.*, 2016, **73**, 293–308.
- 34 H. E. Koschwanez and W. M. Reichert, *Biomaterials*, 2007, **28**(25), 3687–3703.
- 35 J. D. Young, J. Martel, L. Young, C. Y. Wu, A. Young and D. Young, *PLoS One*, 2009, **4**(2), e4417.
- 36 M. Malik, V. Narwal and C. S. Pundir, *Process Biochem.*, 2022, **118**, 11–23.
- 37 T. Deis, K. Rossing, M. K. Ersbøll, E. Wolsk and F. Gustafsson, *Open Heart*, 2022, **9**, e002092.
- 38 B. Yu, Y. Ju, L. West, Y. Moussy and F. Moussy, *Diabetes Technol. Ther.*, 2007, **9**(3), 265–275.
- 39 D. A. Gough, L. S. Kumosa, T. L. Routh, J. T. Lin and J. Y. Lucisano, *Sci. Transl. Med.*, 2010, **2**(42), 42–53.
- 40 M. S. Boyne, D. M. Silver, J. Kaplan and C. D. Saudek, *Diabetes*, 2003, **52**(11), 2790–2794.

